

# Investigating Dark Matter signatures at FCC-ee

by

Asmaa Al-Mellah

IRSRA

# Introduction

- Direct evidence that the **SM** is **not a complete theory** of particle physics:
- The **lack** of a **candidate** for **Dark Matter** (DM).
- These instances of (NPBSM) are exemplified by the **Scotogenic Model**.
- From this point, more prominent windows into **New Physics Beyond the SM (NPBSM)** when the **Large Hadron Collider (LHC)** at CERN has been

Commenced:

**Higgs discovery** and **collider anomalies**

The Higgs physics has witnessed a continuous expansion

# Motivation of our Study

The process  $e^+e^- \rightarrow H^+H^-$  can be used to search possible collider signatures taking into account :

- observations like **dark matter relic density measurement that** has been **updated** in the recent years.

Having updated constraints:

- Allows us to give correct predictions of the **cross section** of the process  $e^+e^- \rightarrow H^+H^-$  in the next run of FCC-ee at CERN,
- The produced  **$H^+H^-$  pair** can **decay** to many final states with different combinations of particles including dark matter candidates under scotogenic model.
- One **common effect** for all such **decay modes** is the **size of the cross section** of  $e^+e^- \rightarrow H^+H^-$ .

# Scotogenic Model

- considered one of the **simplest** and **viable** solutions that accommodates essential elements for **NPBSM**.
- In this model neutrinos acquire **mass** through **radiative processes** involving **one-loop interactions** with **nonstandard particles**.
- New particles :
  - consist of both **fermions** in addition to **scalars**,
  - **lightest** one serving as **DM candidate**.

- three singlet Majorana fermions, denoted as  $N_{1,2,3}$ .
- an additional scalar doublet referred to as  $\eta$  among the inert scalar doublets.
- Furthermore, a  $Z_2$  symmetry, for which, the new added fields will be odd in contrast with particles in SM will remain even.

- the **Lagrangian** describing the **scalar sector** of the Scotogenic model can be written as:

$$\mathcal{L} = (\mathcal{D}^\mu \Phi)^\dagger \mathcal{D}_\mu \Phi + (\mathcal{D}^\mu \eta)^\dagger \mathcal{D}_\mu \eta - \mathcal{V}$$

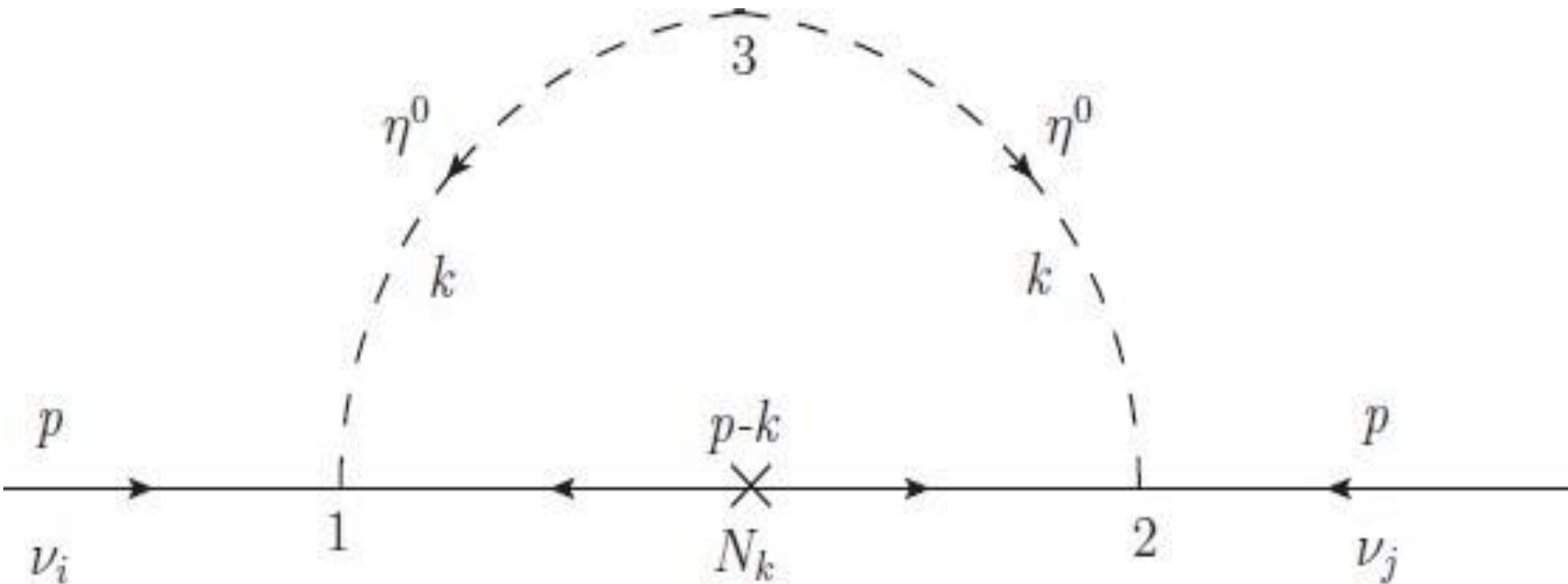
- the **Lagrangian** for the **new singlet Majorana fermions** of the Scotogenic model can be written as:

$$\mathcal{L}_N = -\frac{1}{2} M_k \overline{N_k^c} P_R N_k + Y_{rk} \bar{\ell}_r H^- P_R N_k + \text{H.c.}$$

to masses of  $N_k$ . the  $c$  for  $N_k$  is the charge conjugation of the field.

# Generation of Neutrino Mass in Scotogenic Model

- **neutrinos** exist in **three** flavor states denoted as  $\nu_\alpha$ , where  $\alpha = e, \mu, \tau$ .
- The **masses** of these neutrinos can be generated at the **one-loop level** with internal S, P, and  $N_k$  through Figure.



- The **mass eigenvalues**  $m_j$  are expressed as follows:

$$\text{diag}(m_1, m_2, m_3) = U^\dagger M_\nu U^*$$

- depending on the **neutrino mass** eigenvalues, we get the **mass** for the **neutrinos**:

$$m_1 = \frac{\Lambda_1 y_{e1}^2 e^{-i\alpha_1}}{c_{12}^2 c_{13}^2}, \quad m_2 = \frac{\Lambda_2 y_{e2}^2 e^{-i\alpha_2}}{s_{12}^2 c_{13}^2}, \quad m_3 = \frac{\Lambda_3 y_3^2}{c_{13}^2 c_{23}^2}.$$

- The **experimental** results does **not** give us the **exact** mass of neutrinos but give us the **difference** between their masses.



# Dark Matter in the Scotogenic Model

- In our study, we **adopt** the familiar scenario.
  - We take the  $N_1$  as the **DM particle**.
  - For  $N_2$ , we set it as the **2nd lightest particle** that **degenerate in mass** with  $N_1$

- The **relic density** ( $\Omega \hat{h}^2$ ) is introduced in terms of the **DM density** relative to its critical value, denoted by  $\Omega$ , and the **Hubble parameter**, denoted by  $\hat{h}$ , as  $\Omega \hat{h}^2$ . Theoretically, it can be estimated from the relation:

$$\Omega \hat{h}^2 = \frac{1.07 \times 10^9 x_f \text{ GeV}^{-1}}{\sqrt{g_*} m_{\text{Pl}} [a + 3(b - a/4)/x_f]}$$

- In **our** analysis of the resultant constraint, from the **measured value for DM relic density**, on the parameter space of the model under concern, we consider the case that the **DM** and the **new scalar particles** are **not degenerate** in mass to avoid the contributions of the coannihilation processes of the scalars to the relic density.

## Constraints

- In our analysis, **sum of the neutrino masses** constraint  $\Sigma m_i < 0.12 \text{ eV}$ .
- **neutrino oscillations ratio** based on the 90% CL ranges of the data on

$$32.0 < \frac{|\Delta m_{31}^2|}{\Delta m_{21}^2} < 36.0$$

- The **limits** from **up to date-experimental data** on **LFV** processes are

$$\text{BR}(\mu \rightarrow e\gamma) < 4.2 \times 10^{-13}$$

- The flavor-diagonal counterpart of the previous **LFV** processes leads to a modification of the **anomalous magnetic moment**  $a_{\ell_i}$  of the **lepton**  $\ell_i$  given by:

$$\Delta a_{\ell_i} = \frac{-m_{\ell_i}^2}{16\pi^2 m_H^2} \sum_k |y_{ik}|^2 \mathcal{F}(M_k^2/m_H^2)$$

- For the **DM candidate**  $N_1$ , the interactions with nucleons appear at the one-loop level.
- set the **couplings**  $\lambda_{3,4} = 0.01$  to avoid the strong constraints from **direct detection**.
- from the discussion about **scalar masses** we find that:  

$$m_0 \simeq m_S \simeq m_P \simeq m_{H^\pm} + \frac{1}{2}\lambda_4 v^2 \simeq m_{H^\pm} + 350 \text{ GeV}.$$
- It should be noted that the **strong constraints** from the **direct detection** were **not studied before**.
- In **our** study, we **first** to allocate the **mixing angles**  $\theta_{12,23,13}$  and the **Dirac phase**  $\delta$  to their central values got in the fit to the global data on neutrino oscillation.

- In the **second** step, we apply a scan over the parameter space of the model recognized, the **masses** of the **new scalars**  $m_H$ ,  $m_0$  and the **new singlet fermions**  $N_{1,2,3}$  and the input parameters  $Y_{1,2,3}$  appearing in the Yukawa couplings.
- For **light dark matter masses**  $M1 < 100$  GeV, LFV and direct search at LHC:

Experimentally, **constraints** can be set on the **masses** of the **new** scalars using the data on  $W$  and  $Z$  widths and the null results of **direct searches** for **new particles** at  $e^+e^-$  colliders:

$$m_{H^\pm} + m_{S,P} > m_{W^\pm}, m_{H^\pm} > 70 \text{ GeV}, m_S + m_P > m_Z,$$

# Cross Section of $e^+e^- \rightarrow H^+H^-$

- The cross section of our process  $e^+e^- \rightarrow H^+H^-$  in the FCC-ee is given by :

$$\begin{aligned}
 \sigma_{e\bar{e} \rightarrow H\bar{H}} = & \frac{\pi \alpha^2 \beta^3}{3s} + \frac{\alpha}{12} \frac{(g_L^2 + g_L g_R) \beta^3}{s - m_Z^2} + \frac{(g_L^4 + g_L^2 g_R^2) \beta^3 s}{96\pi (s - m_Z^2)^2} + \sum_k \frac{|\dagger_{1k}|^4}{64\pi s} \left( w_k \ln \frac{w_k + \beta}{w_k - \beta} - 2\beta \right) \\
 & + \left[ \frac{\alpha}{16s} + \frac{g_L^2}{64\pi (s - m_Z^2)} \right] \sum_k |\dagger_{1k}|^2 \left[ (w_k^2 - \beta^2) \ln \frac{w_k + \beta}{w_k - \beta} - 2\beta w_k \right] \\
 & + \sum_{j,k>j} \frac{|\dagger_{1j} \mathcal{Y}_{1k}|^2}{64\pi s} \left( \frac{w_j^2 - \beta^2}{w_j - w_k} \ln \frac{w_j + \beta}{w_j - \beta} + \frac{w_k^2 - \beta^2}{w_k - w_j} \ln \frac{w_k + \beta}{w_k - \beta} - 2\beta \right), \tag{4.14}
 \end{aligned}$$

# Results and Discussion

- We start first by showing the **effect** of the different **constraints** on the parameter space of the **model**.
- The allowed parameter space of the scotogenic model is determined by the **regions** in the  $(M_1, M_2, M_3, m_0, m_H, y_1, y_2, y_3)$  plane satisfying all the **strong constraints**.
- We consider **two** scenarios depending on the values of  $M_1$  and  $M_2$ .
  - In the **first** one, we take  $M_3 > M_2 > M_1$
  - In the **second** scenario,  $M_2 \simeq M_1$  which is favored:  
to allow simultaneous **satisfaction** of **constraints** from **dark matter** relic density and branching ratio of  $\mu \rightarrow e\gamma$ .

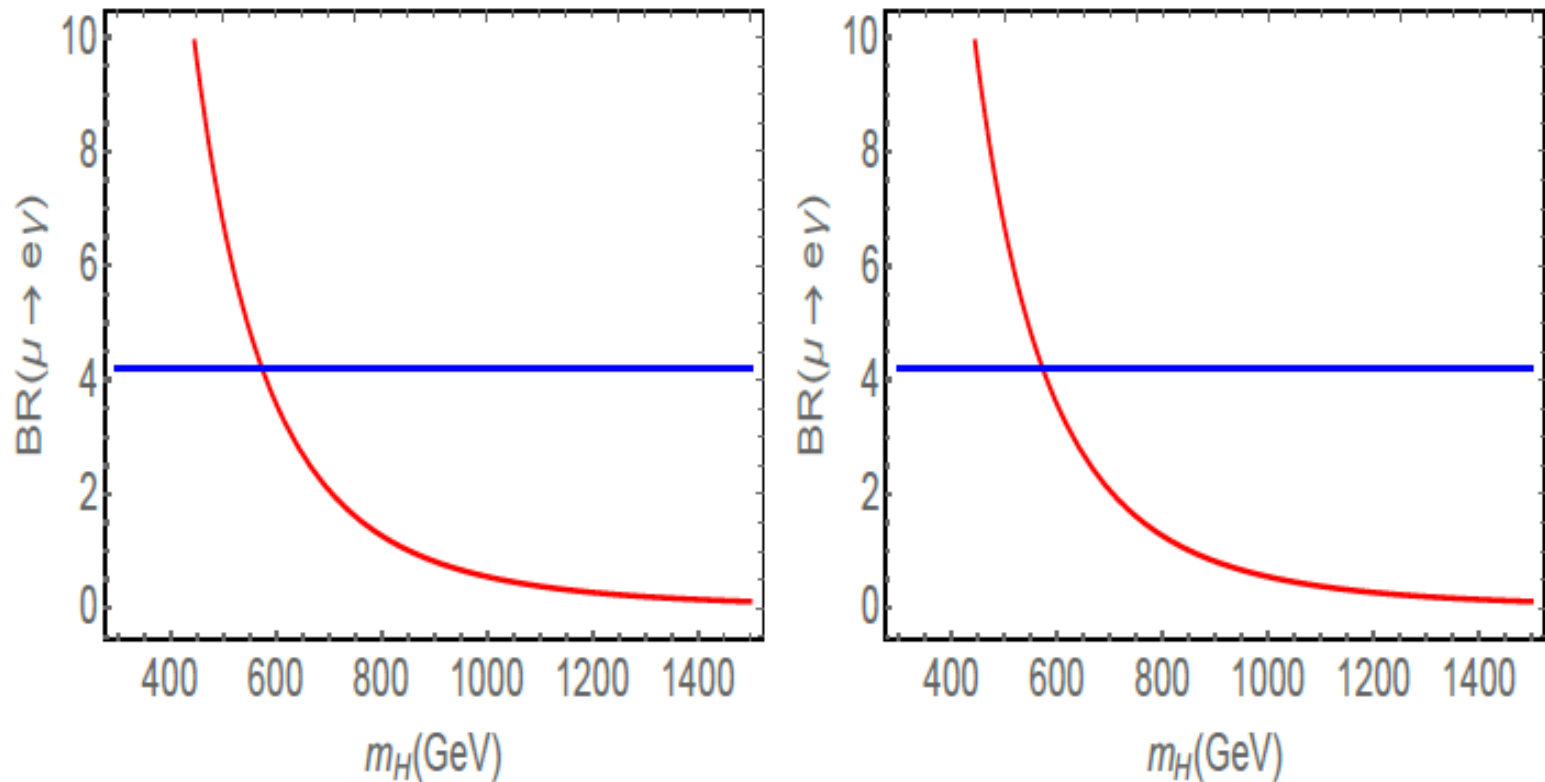


Figure 5.1. Left (Right) plot:  $BR(\mu \rightarrow e\gamma)$  in units of  $10^{-13}$  in red color as a function of  $m_H$  in the first (second) scenario. For the left plot we impose  $M_1 = 200$  GeV,  $M_2 = M_1 + 100$  GeV,  $M_3 = M_1 + 200$  GeV,  $y_1 = 0.03, y_2 = 0.01, y_3 = 0.02$ , and for the right one we set  $M_1 = M_2 = 200$  GeV,  $M_3 = M_1 + 200$  GeV,  $y_1 = 0.03, y_2 = 0.01, y_3 = 0.02$ . The blue line represent the experimental upper bound on  $BR(\mu \rightarrow e\gamma)$ .



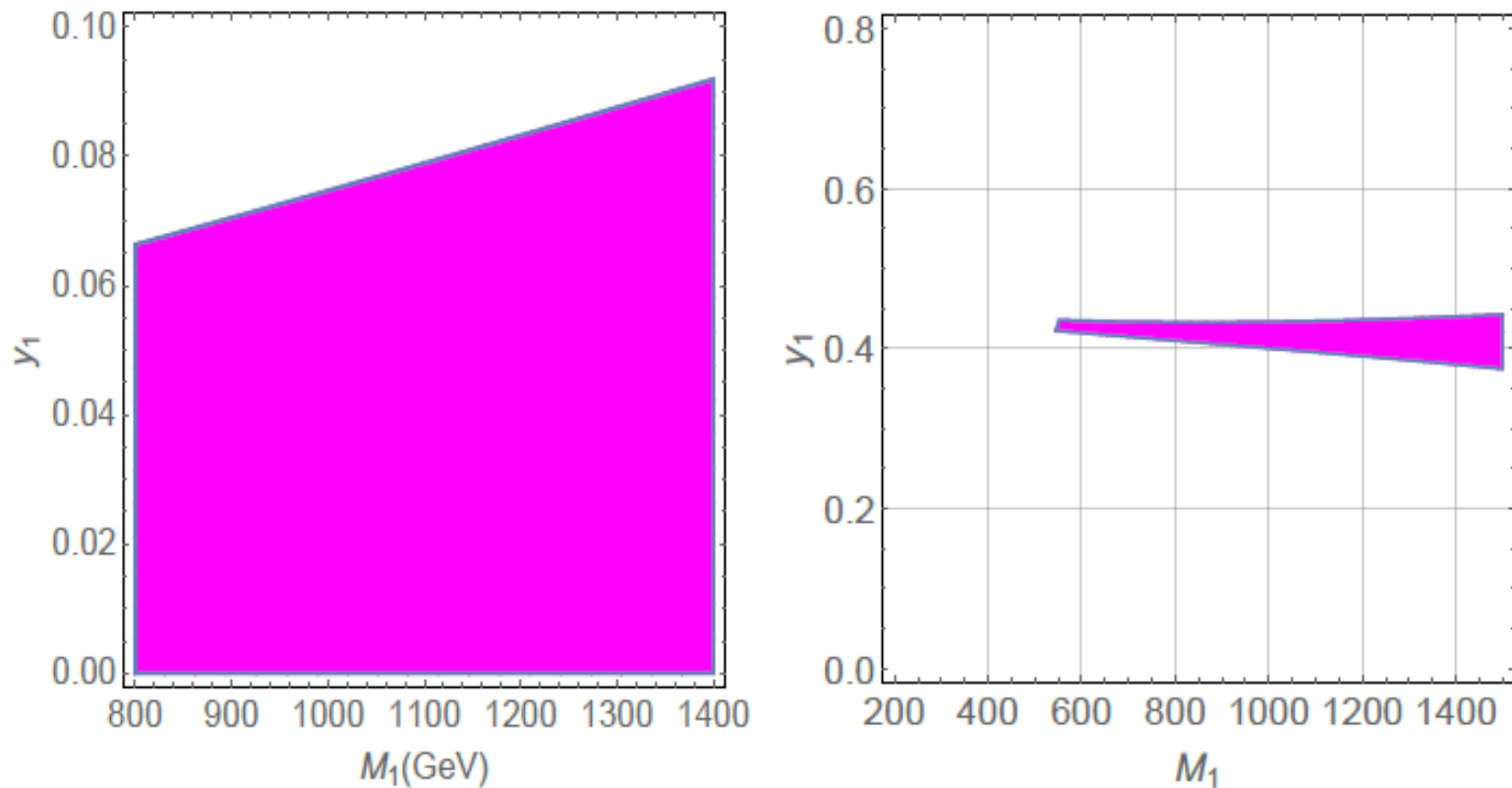


Figure 5.2. Left (Right) plot: regions in magenta color satisfying the constraints  $BR(\mu \rightarrow e\gamma) < 4.2 \times 10^{-13}$ . The left plot is obtained after setting  $M_2 = M_1 + 100$  GeV,  $m_H = M_1 + 400$  GeV,  $M_3 = M_1 + 200$  GeV,  $y_2 = 0.01$ ,  $Y_3 = 0.02$  where the right one is obtained upon taking  $M_2 = M_1$  GeV,  $M_3 = M_1 + 1370$  GeV,  $y_2 = 0.49$ ,  $y_3 = 0.66$ .

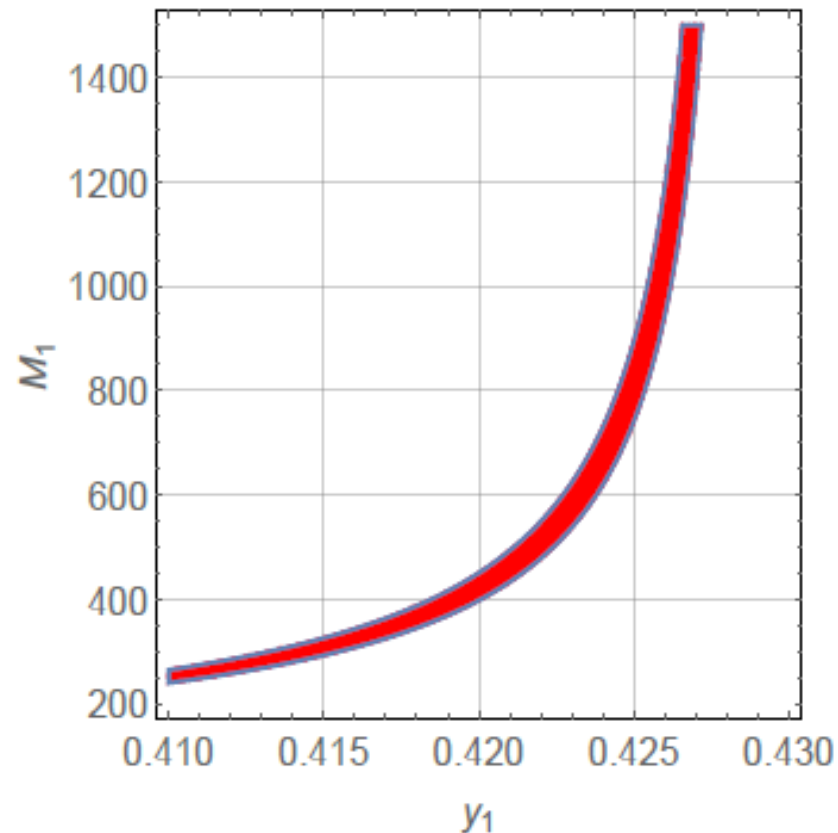
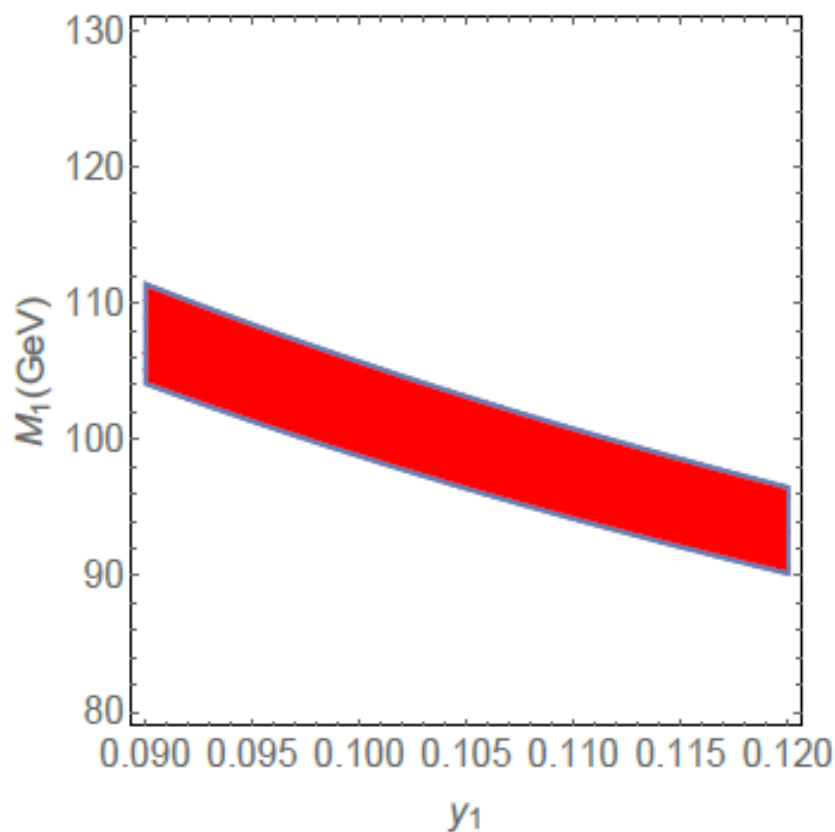


Figure 5.3. left (Right) plots, allowed region in  $M_1 - y_1$  plane satisfying the constraint  $32 < R_m < 36$  corresponding to first(second) scenario mentioned before. We took  $m_0 = M_1 + 500$  GeV,  $M_2 = M_1 + 50$  GeV,  $M_3 = M_1 + 170$  GeV,  $y_2 = 0.2, Y_3 = 0.3$  to obtain the left plot where for the right plot we set  $M_2 = M_1$  for  $M_3 = M_1 + 380$  GeV,  $m_0 = M_1 + 750$ ,  $y_2 = 0.49, y_3 = 0.66$ .

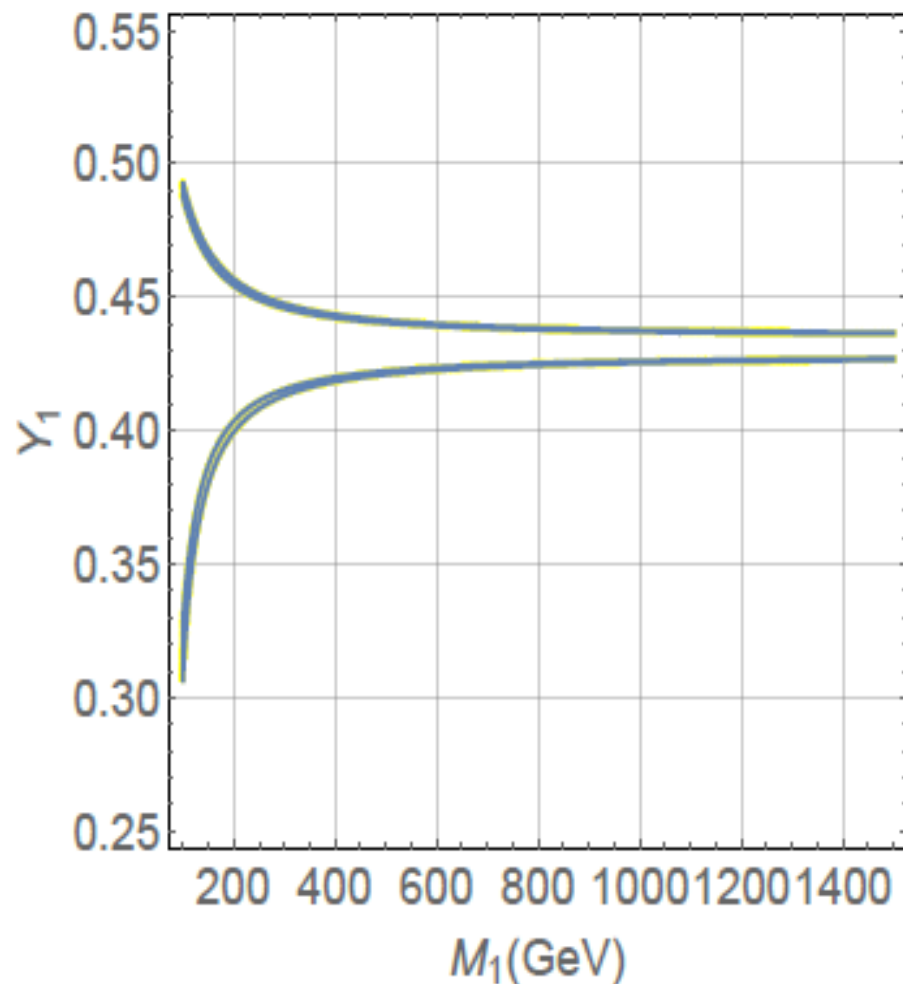


Figure 5.4. Allowed regions in the  $M_1 - y_1$  plane after imposing  $32 < R_m < 36$  constraints for the choice of the parameters as  $M_2 = M_1$ ,  $M_3 = M_1 + 380$  GeV,  $m_0 = M_1 + 750$  GeV,  $y_2 = 0.49$  and  $y_3 = 0.66$ .

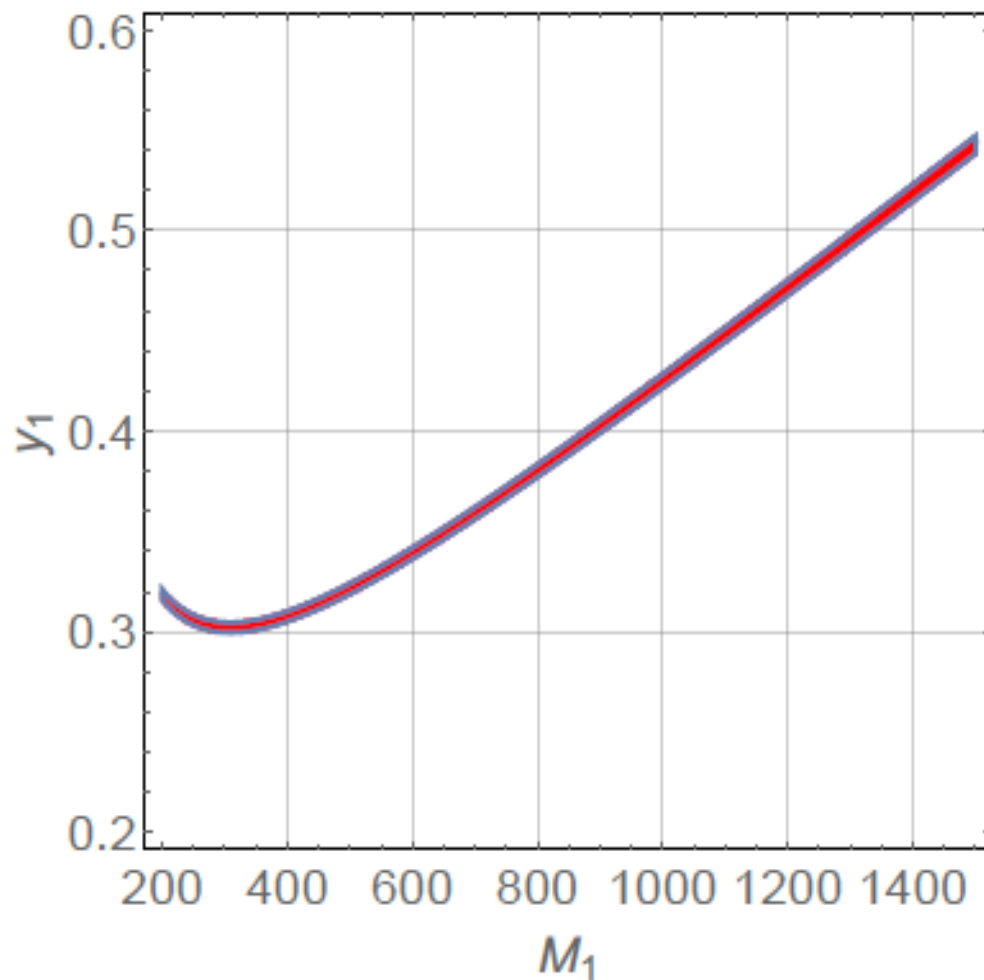


Figure 5.5. Allowed region in  $M_1 - y_1$  plane satisfying the  $0.118 \leq \Omega_{\hat{h}}^2 \leq 0.122$  for  $m_0 = M_1 + 750$  GeV,  $m_H = M_1 + 400$  GeV,  $g_s = 100$ ,  $y_2 = 0.49$  .

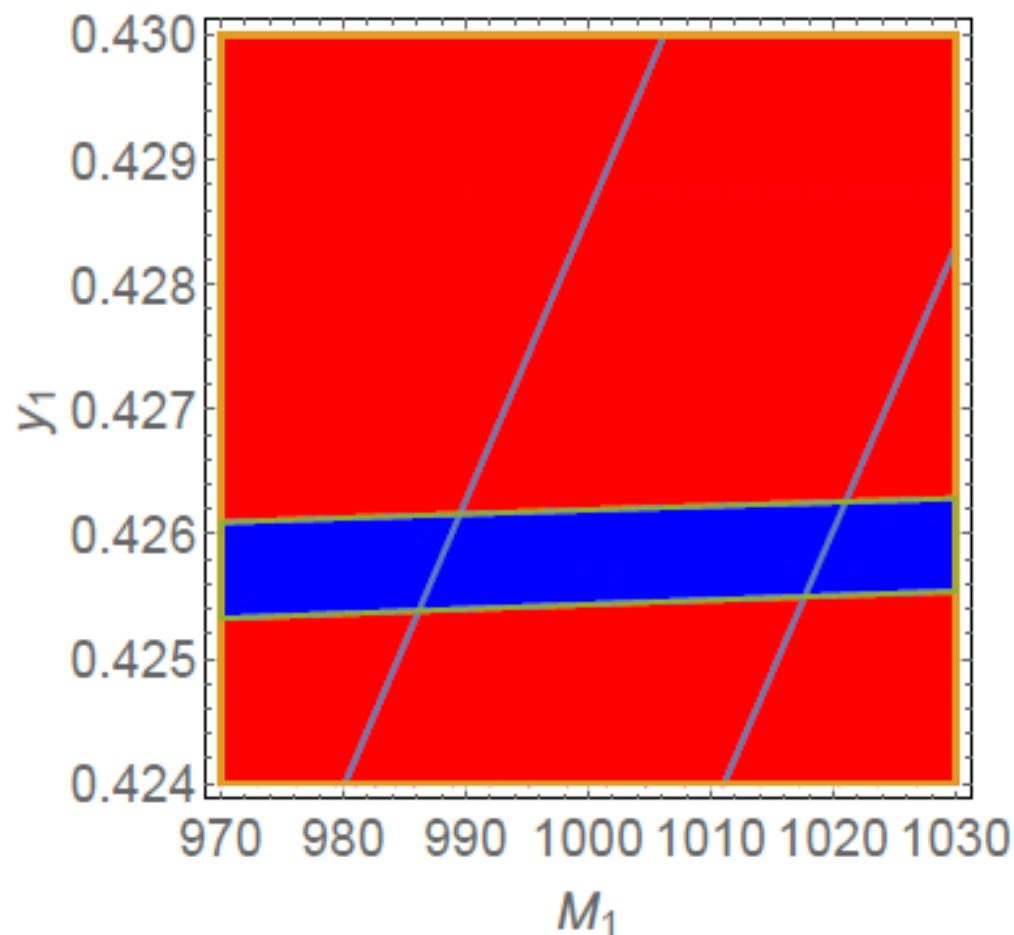


Figure 5.6. Allowed region in  $M_1 - y_1$  plane satisfying our constraints  $0.118 \leq \Omega_{\hat{h}}^2 \leq 0.122$ ,  $BR(\mu \rightarrow e\gamma) < 4.2 \times 10^{-13}$  and  $32 < R_m < 36$ . for  $m_0 = M_1 + 750$  GeV,  $m_H = M_1 + 400$  GeV,  $g_s = 100$ ,  $M_3 = M_1 + 380$  GeV,  $y_2 = 0.49$ ,  $y_3 = 0.66$ .

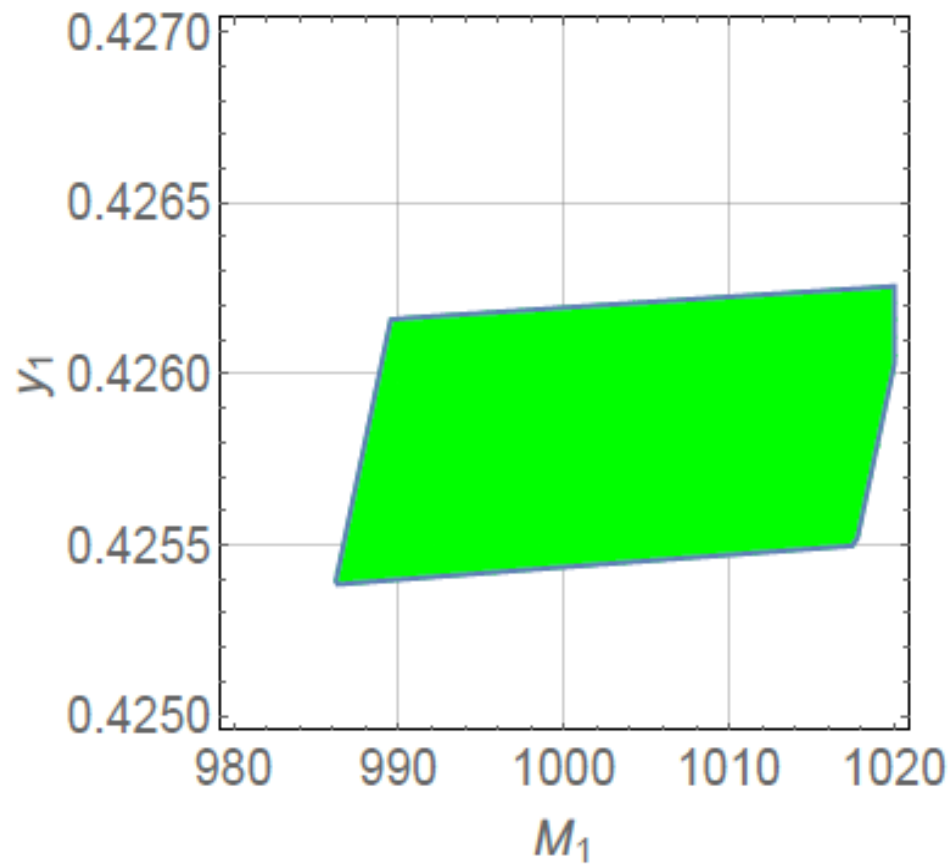


Figure 5.7. Allowed region in  $M_1 - y_1$  plane interaction point for  $0.118 \leq \Omega_{\hat{h}}^2 \leq 0.122$ ,  $BR(\mu \rightarrow e\gamma) < 4.2 \times 10^{-13}$  and  $32 < R_m < 36$ , for  $m_0 = M_1 + 750$  GeV,  $m_H = M_1 + 400$  GeV,  $g_s = 100$ ,  $M_3 = M_1 + 380$  GeV,  $y_2 = 0.49$ ,  $y_3 = 0.66$ .

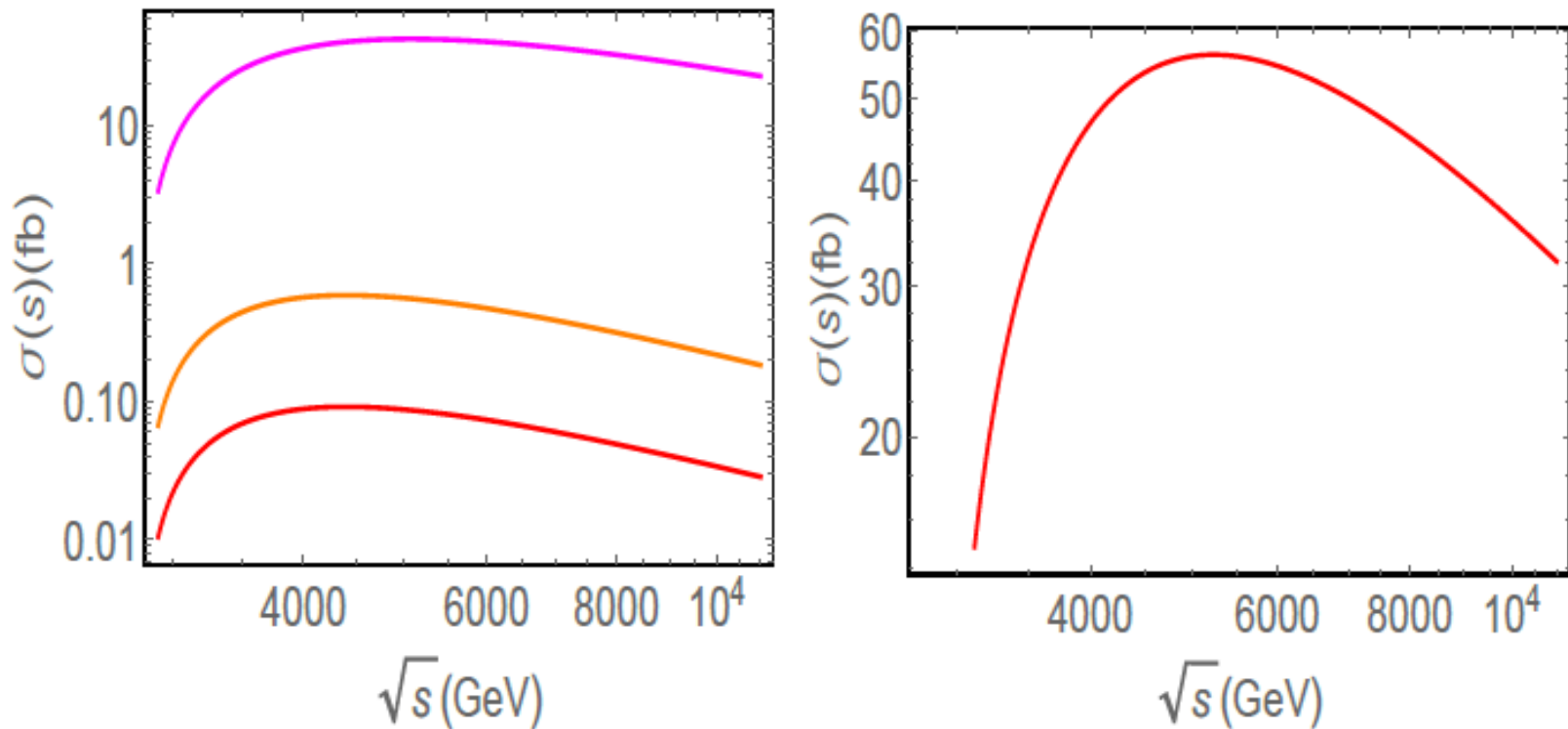


Figure 5.8. Left: photon, Z boson and singlet fermions  $N_{1,2,3}$  contributions to the cross section for the process  $e^+e^- \rightarrow H^+H^-$  in orange, red and magenta colors respectively as a function of  $\sigma(s)$  (fb) –  $\sqrt{s}$ (GeV) for  $m_H = M_1 + 400$  GeV,  $M_1 = 990$  GeV,  $M_2 = M_1 + 0.0000035$  GeV,  $M_3 = M_1 + 380$  GeV,  $y_1 = 0.4258$ ,  $y_2 = 0.49$ ,  $y_3 = 0.66$ , Right: total cross section for the process  $e^+e^- \rightarrow H^+H^-$  in red color as a function of  $\sigma(s)$  (fb) –  $\sqrt{s}$ (GeV) for  $m_H = M_1 + 400$  GeV,  $M_1 = 990$  GeV,  $M_2 = M_1 + 0.0000035$  GeV,  $M_3 = M_1 + 380$  GeV,  $y_1 = 0.4258$ ,  $y_2 = 0.49$ ,  $y_3 = 0.66$  .

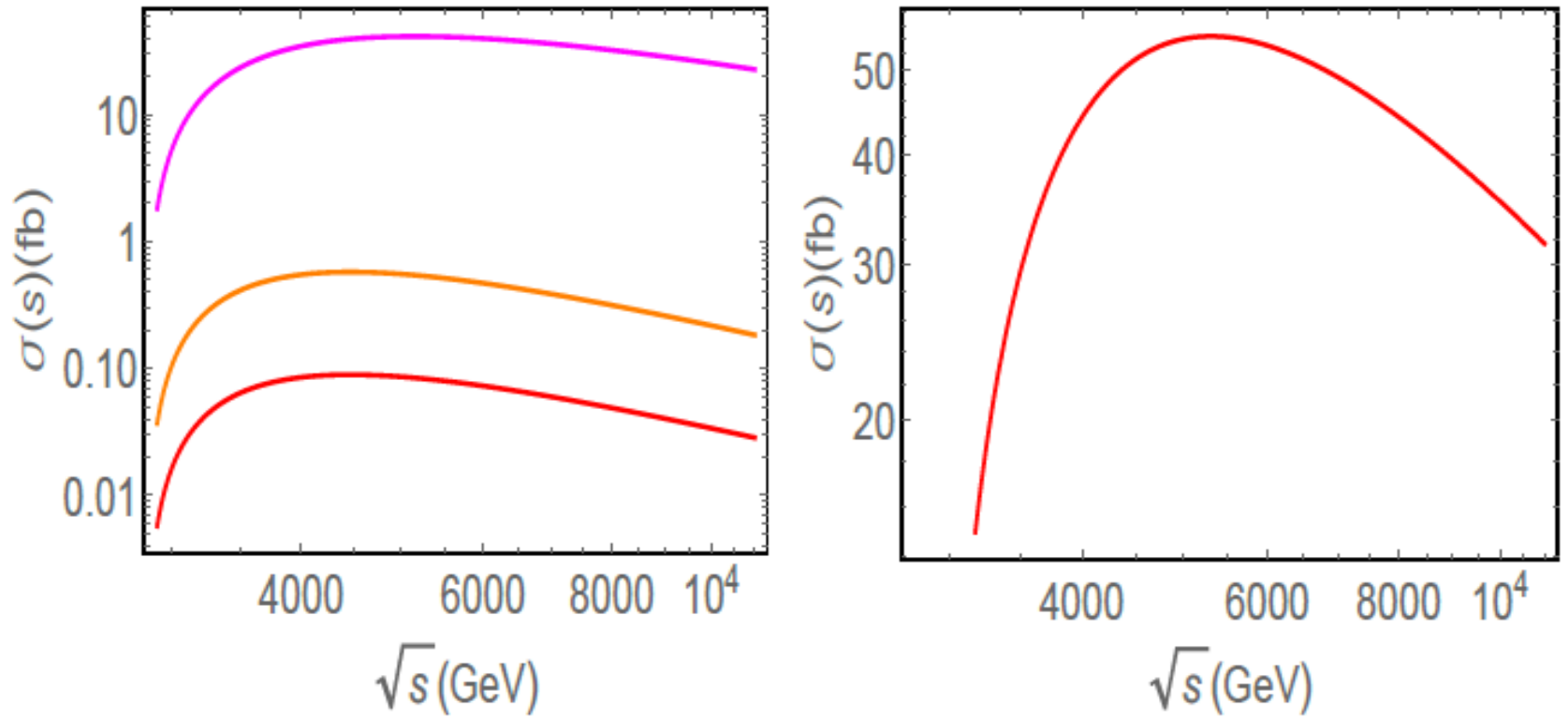


Figure 5.9. Left: photon, Z boson and singlet fermions  $N_{1,2,3}$  contributions to the cross section for the process  $e^+e^- \rightarrow H^+H^-$  in orange, red and magenta colors respectively as a function of  $\sigma(s)$  (fb) –  $\sqrt{s}$ (GeV) for  $m_H = M_1 + 400$  GeV,  $M_1 = 1010$  GeV,  $M_2 = M_1 + 0.0000035$  GeV,  $M_3 = M_1 + 380$  GeV,  $y_1 = 0.4258$ ,  $y_2 = 0.49$ ,  $y_3 = 0.66$ . Right: total cross section for the process  $e^+e^- \rightarrow H^+H^-$  in red color as a function of  $\sigma(s)$  (fb) –  $\sqrt{s}$ (GeV) for  $m_H = M_1 + 400$  GeV,  $M_1 = 1010$  GeV,  $M_2 = M_1 + 0.0000035$  GeV,  $M_3 = M_1 + 380$  GeV,  $y_1 = 0.4258$ ,  $y_2 = 0.49$ ,  $y_3 = 0.66$ .



# CONCLUSIONS

- we have **studied** the process  $e^+e^- \rightarrow H^+H^-$  in the scotogenic model.
- The different contributions to the amplitude of the process originate from **tree-level diagrams** mediated by **photon**, **Z boson** and from the **right-handed fermions**  $N_{1,2,3}$ .
- We have **studied** the **processes** with **strong constraints** on the parameter space relevant to the process  $e^+e^- \rightarrow H^+H^-$ .
- we have **estimated** the **size** of the individual **contributions** of each of **photon**, **Z boson** and the **right-handed fermions**  $N_{1,2,3}$  to the **cross section** of  $e^+e^- \rightarrow H^+H^-$  after taking into account all stringent constraints on the parameters of the model.

- We have **shown** that the main **contribution** to the **cross section** arise from the **new** singlet right handed fermions  $N_{1,2,3}$ .
- Finally, we have shown the **dependency** of the **cross section** on the **center of mass** energy for set of benchmark points of the parameter space of the model respecting the strong obtained bounds.
- **Future  $e^+e^-$  colliders** will search for the process  $e^+e^- \rightarrow H^+H^-$  and thus **can test our predictions** for either verifying these predictions or setting more stringent constraints.

Thank you  
for  
listening 😊